Available online at www.sciencedirect.com

SCIENCE DIRECT

Virology 348 (2006) 418–429

VIROLOGY

www.elsevier.com/locate/yviro

Downregulation of human immunodeficiency virus type 1 Gag expression by a gp41 cytoplasmic domain fusion protein

Woan-Eng Chan, Steve S.-L. Chen *

Institute of Biomedical Sciences, Academia Sinica, No. 128 Yen-Chiu-Yuan Road, Section 2, Nankang, Taipei 11529, Taiwan, Republic of China

Received 1 September 2005; returned to author for revision 21 October 2005; accepted 6 January 2006
Available online 9 February 2006

Abstract

The cytoplasmic domain of human immunodeficiency virus type 1 (HIV-1) envelope (Env) transmembrane protein gp41 interacts with the viral matrix MA protein, which facilitates incorporation of the trimeric Env complex into the virus. It is thus feasible to design an anti-HIV strategy targeting this interaction. We herein describe that Gag expression can be downregulated by a cytoplasmic domain fusion protein of the Env transmembrane protein, β-galactosidase (β-gal)/706–856, which contains the cytoplasmic tail of gp41 fused at the C terminus of *Escherichia coli* β-gal. This mediator depleted intracellular Gag molecules in a dose-dependent manner. Sucrose gradient ultracentrifugation and confocal microscopy revealed that Gag and β-gal/706–856 had stable interactions and formed aggregated complexes in perinuclear, intracellular sites. Pulse-chase and cycloheximide chase analyses demonstrated that this mediator enhanced unmyristylated Gag degradation. The results demonstrate a novel mode of HIV-1 Gag downregulation by directing Gag to an intracellular site via the interaction of Gag with a gp41 cytoplasmic domain fusion protein.

Keywords: HIV-1; gp41; Cytoplasmic domain; Gag; Gag-cytoplasmic domain interaction; Anti-HIV-1 strategy; Gag downregulation; Degradation; Colocalization

Introduction

The assembly of human immunodeficiency virus type 1 (HIV-1), HIV-2, and simian immunodeficiency virus (SIV), all lentiviruses, is directed by the Gag protein, which contains all of the determinants necessary and sufficient for viral assembly and budding (for reviews see references Freed, 1998; Garnier et al., 1998; Sakalian and Hunter, 1998). Formation of infectious HIV and SIV particles involves incorporation of viral envelope (Env) glycoproteins as well as viral RNA into the nascent particles that bud from the cell surface. During virus assembly and morphogenesis, the Gag polyproteins assemble into a network of "ring-like" structures at the plasma membrane; following proteolytic cleavage of the Gag precursor, the mature capsid (CA) protein forms a "fullerene-like" shell of the viral core (Gelderblom et al., 1987; Nermut et al., 1994). Also, within the maturing viral particle, the matrix (MA) protein remains in the inner face of the virion envelope and is associated with the lipid bilayer by the myristic acid attached to its N-terminus. The basic multimeric unit of the MA protein is a trimer (Massiah et al., 1994; Matthews et al., 1994; Rao et al., 1995), and this model proposes that the cytoplasmic tail of the trimeric Env is localized to the cage hole present in the lattice-like MA structure formed upon MA trimerization (Hill et al., 1996).

During maturation, assembly, and budding processes, Pr55 Gag complexes are present as large, intermediate multimeric assembly complexes in the cytoplasm as well as membrane fractions of infected cells (Ono and Freed, 1999; Paillart and Gottlinger, 1999; Spearman et al., 1997). Further kinetic analyses of Gag synthesis and assembly demonstrated that newly synthesized Gag molecules rapidly form detergent-resistant, cytoplasmic Gag complexes and that a subpopulation of newly synthesized Gag can be chased into membrane-bound complexes of increasing size or density over the chase period (Tritel and Resh, 2000). Also, a major fraction of newly synthesized Gag may undergo proteasomal degradation, presumably due to misfolding of the Gag molecules (Schubert et al., 2000; Tritel and Resh, 2000).

* Corresponding author. Fax: +886 2 2785 8847.
E-mail address: schen@ibms.sinica.edu.tw (S.S.-L. Chen).

0042-6822/$ - see front matter © 2006 Elsevier Inc. All rights reserved.
doi:10.1016/j.virol.2006.01.010

Extensive studies have revealed that the Env–MA interaction facilitates recruitment of the trimeric Env complex into buds where mature virions are released into the medium (for reviews see references Freed, 1998; Garoff et al., 1998). The intracellular targeting and localization properties of Gag and Env are often affected by alterations in their counterparts (Hermida-Matsumoto and Resh, 2000; Vincent et al., 1999), nevertheless, Salzwedel et al. (1998) showed that retention of the Env protein in the endoplasmic reticulum (ER) by adding an ER retention signal to the C terminus of the protein neither affects Gag intracellular localization nor alters Gag budding from the plasma membrane. Other studies have also substantiated the notion that interactions between the transmembrane gp41 protein and Gag are specific for the presence of the cytoplasmic tail of gp41 (Cosson, 1996; Vincent et al., 1999; Wyma et al., 2000).

The cytoplasmic domain of gp41, encompassing residues 706 to 856, is characterized by the presence of three amphipathic α-helical segments, located at residues 828–856, 770–795, and 789–815, respectively, at its C-terminus. Due to their cytolytic effects on cell membranes, these three motifs are referred to as the lentivirus lytic peptide (LLP)-1, LLP-2, and LLP-3, respectively. The cytoplasmic tail has been shown to interact with various cellular components, such as proteins involved in the induction of apoptosis (Micoli et al., 2000; Pan et al., 1996), the AP-1 and AP-2 clathrin–adaptor complexes (Berlioz-Torrent et al., 1999; Boge et al., 1998; Ohno et al., 1997; Wyss et al., 2001), and TIP47, a protein required for the transport of mannose-6-phosphate receptors from endosomes to the *trans*-Golgi network (Blot et al., 2003). Our previous studies supported the proposal that the oligomerization and membrane-binding abilities of the cytoplasmic domain play crucial roles in Env assembly and virus infection (Chen et al., 1996, 1999, 2001; Lee et al., 2000). It is conceivable that Gag-cytoplasmic tail interaction can be used as a strategic target for the design of an anti-HIV strategy.

Since Gag is an attractive target for designing anti-HIV strategies, it is of interest to understand whether Gag expression can somehow be downregulated in Gag expression cells. We demonstrate herein that *Escherichia* (*E.*) *coli* β-galactosidase (β-gal) and a cytoplasmic tail fusion protein, β-gal/706–856, acts as a novel modulator to abrogate steady-state Gag expression via degradation. Also, the cytoplasmic tail fusion protein specifically interacts with Gag and directs Gag to an intracellular site. To our knowledge, this mode of down-regulation of HIV-1 Gag expression has never been noted in previously reported HIV dominant-negative mutants or anti-HIV strategies. Our study also has implications in devising a genetic anti-HIV approach to interfering with Gag maturation.

Results

Downregulation of HIV-1 Gag expression by a gp41 cytoplasmic tail fusion protein

To explore whether the interaction of the cytoplasmic tail of gp41 with Gag can serve as a strategic target for the development of an anti-HIV-1 approach, we examined whether a cytoplasmic domain fusion protein expressed in cells can affect steady-state Gag expression. 293T cells were cotransfected with equal amounts of pHIVgpt and pCDNA3-β-gal/706–856. pHIVgpt encodes an HIV genome in which the *env* gene is replaced by an simian virus (SV) 40 promoter-driven *gpt* gene (Page et al., 1990). pCDNA3-β-gal/706–856 encodes the entire cytoplasmic tail of the HXB2 strain Env fused to the C terminus of the *E. coli* reporter protein β-gal (Chen et al., 2001). Cotransfection with pCDNA3 or pCDNA3-β-gal was used as negative controls. Equal volumes of cell and virion lysates were resolved by sodium dodecyl sulfate (SDS)-polyacrylamide gel electrophoresis (PAGE) followed by Western blotting using mouse monoclonal antibody (Mab) 183, which is specific the p24 CA protein. During or after virus budding, the Pr55 Gag precursor is cleaved by the virus-encoded protease into MA p17, CA p24, p2 (sp 1), nucleocapsid p7, p1 (sp 2), and the C-terminal p6 domain. With β-gal/706–856 coexpression, the intracellular levels of Pr55, an uncleaved MA and CA intermediate (p41), and p24, which are all recognized by Mab 183, were remarkably reduced compared both to the control, which did not express β-gal, and to β-gal coexpression (Fig. 1A, middle panel, compare lane 4 to lanes 2 and 3). The virion-associated levels of Pr55 and its cleavage products were also strikingly reduced in β-gal/706–856 coexpression (Fig. 1A, middle panel, lane 9). The effect of this mediator on reduced steady-state Gag expression was specific since β-gal/706–752, in which the sequence spanning residues 706 to 752 of Env was fused at the C terminus of β-gal, did not affect Gag expression or budding (Fig. 1A, middle panel, lanes 5 and 10). When samples were analyzed for expression of β-gal or the β-gal fusion proteins, a similar level of β-gal/706–856 was detected in cells compared to β-gal and β-gal/706–752 expression (Fig. 1A, top panel). β-gal/706–856 appeared to be prone to degradation since a smaller-molecular-weight species which co-migrated with β-gal could be detected with β-gal/706–856 coexpression (Fig. 1A, top panel, lane 4).

Effects of Gag structures on β-gal/706–856-modulated Gag expression

To examine whether Gag processing affects β-gal/706–856-modulated Gag expressions, 293T cells were cotransfected with a pHIVgpt-derived pHIVgpt*pro*$^-$ construct and each of the pCDNA3-β-gal plasmids at a 1:1 molar ratio. Since pHIVgpt-*pro*$^-$ encodes a dysfunctional protease in which the catalytic site at residue Asp-25 of the *pro* gene in pHIVgpt is mutated to Asn (Wang et al., 2000), the Pr55 precursor synthesized was not cleaved to produce p41 or p24. Similar levels of β-gal and β-gal/706–856 were expressed in cells (Fig. 1B). Again, β-gal/706–856 significantly reduced the intracellular and virion-associated Pr55 level compared to β-gal coexpression (Fig. 1B).

To study whether Gag targeting to the plasma membrane is crucial for the downregulating effect of β-gal/706–856 on Gag expressions, pHIVgpt*myr*$^-$, which encodes a Gly-to-Ala substitution at residue 2 of MA in the *env*-defective pHIVgpt backbone (Wang and Barklis, 1993), was examined.

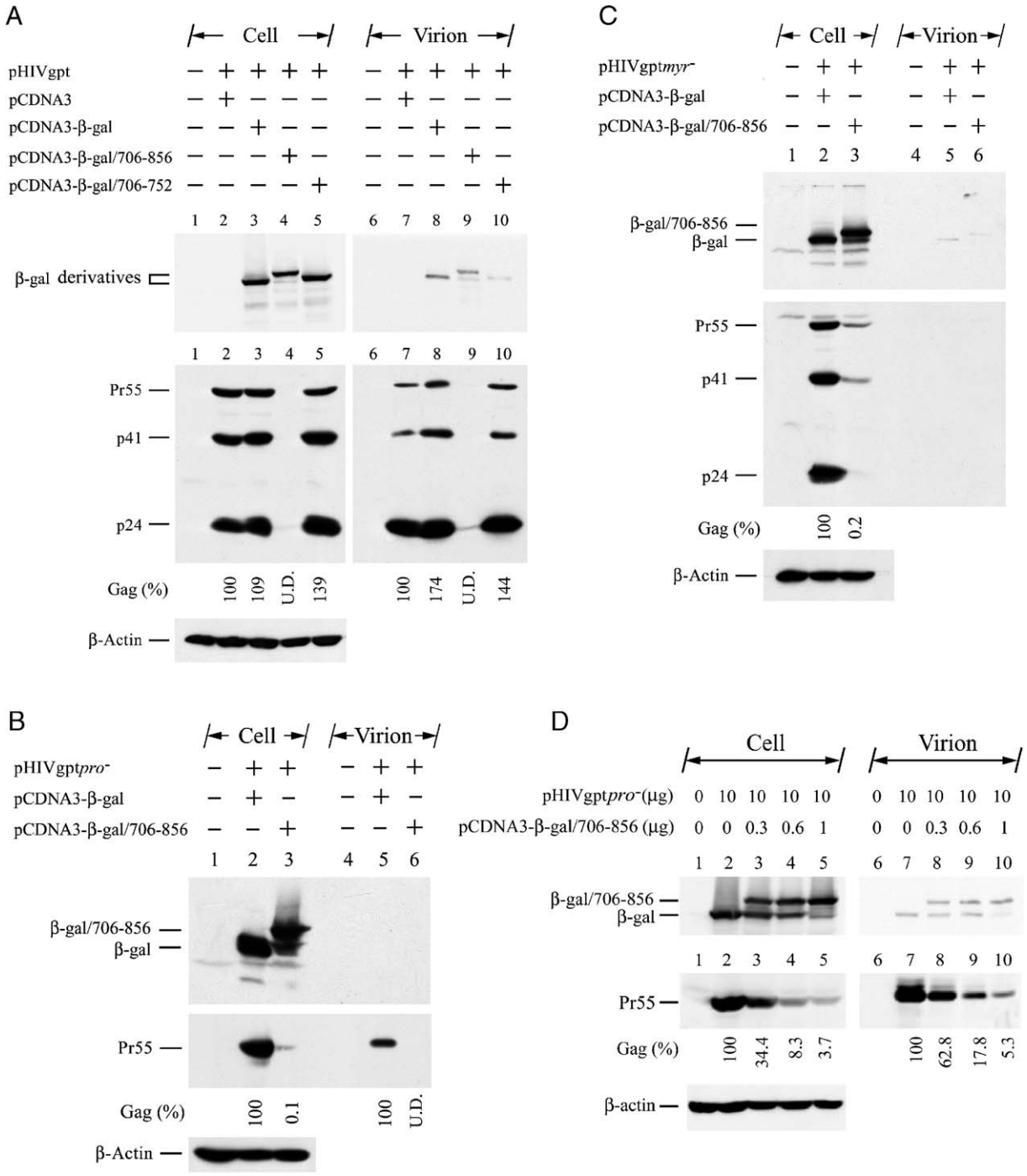

Fig. 1. Reduced Gag expression by β-gal/706–856. 293T cells were cotransfected with each of the pCDNA3 plasmids as indicated along with pHIVgpt (A), pHIVgpt*pro*⁻ (B), or pHIVgpt*myr*⁻ (C), respectively, and Western blotting using Mabs β-gal, 183, and β-actin, respectively, was then performed. In (D), cells were cotransfected with 10 μg of pHIVgptp*ro*⁻ and 5 μg of pRL-TK in the presence of an increasing amount of pCDNA3-β-gal/706–856 as indicated. pCDNA3-β-gal was added to keep the total amounts of the β-gal plasmids in the transfections the same. The relative percentages of Gag in cells and virions are indicated below each of the lanes. U.D., undetectable.

Unmyristylated Gag was barely detected in the culture medium (Fig. 1C, lane 5) since abolishment of the Pr55 myristylation signal by this mutation severely impairs Gag targeting to the plasma membrane, as well as virus assembly and budding (Bryant and Ratner, 1990; Gottlinger et al., 1989; Ono and Freed, 1999; Spearman et al., 1997; Zhou and Resh, 1996). Nevertheless, β-gal/706–856 still greatly depleted the intracellular levels of Gag and its cleavage products (Fig. 1C). As shown in Figs. 1A and B, similar amounts of β-gal and β-gal/706–856 were detected in cells (Fig. 1C).

To further study the specific effect of β-gal/706–856 on Gag expression and to determine whether expression of β-gal/706–856 affects the efficiency of plasmid transfection, 293T cells were cotransfected with fixed amounts of pHIVgpt*pro*⁻ and

pRL-TK along with an increasing amount of pCDNA3-β-gal/706–856. pRL-TK encodes a *Renilla reniformis* luciferase gene under the control of the promoter of the herpes simplex virus thymidine kinase gene. Comparable levels of luciferase activity were detected in each transfection. Also, similar amounts of β-gal and β-gal/706–856 were expressed in cells when equal amounts of β-gal and β-gal/706–856 plasmids were used for transfection (Fig. 1D, compare lanes 2 and 5). β-gal/706–856 decreased Gag expression in a dose-dependent manner (Fig. 1D).

Depletion of both cytosolic and membrane-associated Gag complexes by β-gal/706–856

To determine which population, the membrane-free or membrane-associated Gag proteins in cells, is depleted by the fusion protein, 293T cells cotransfected with pHIVgpt*pro*$^-$ or pHIVgpt*myr*$^-$ together with either the β-gal or β-gal/706–856 plasmid were subjected to a membrane flotation assay. As previously reported (Chen et al., 2001), β-gal was predominantly located in the soluble fractions 1 to 3 while β-gal/706–856 floated to membrane fractions 7 and 8 of the sucrose gradient (data not shown). When coexpressed with β-gal, the majority of myristylated Pr55 Gag molecules were located in the membrane fractions although a small fraction of Gag could be detected in the soluble fraction (Fig. 2, left upper panel). β-gal/706–856 strikingly depleted both the cytosolic and membrane-associated Myr$^+$–Gag proteins (Fig. 2, left bottom panel). As expected, Myr$^-$ Gag was predominantly located in the soluble, cytosolic fractions when coexpressed with β-gal (Fig. 2, right upper panel), while β-gal/706–856 significantly depleted the Gag proteins in these soluble fractions (Fig. 2, right bottom panel).

No measurable effects of β-gal/706–856 on Env expression and cellular functions

To assess whether the depleting effect of β-gal/706–856 on Gag expression was specific for Gag, the effect of this mediator on Env expression was examined. This mediator did not greatly affect steady-state Env expression from an HIV-1 long-terminal-repeat (LTR)-directed *env* plasmid pSVE7*puro* (Fig. 3A), nor did it alter the steady-state Env expression from pBSX, an SV40 promoter-driven *env* plasmid, even at a 1:2 molar ratio of *env* to β-gal/706–856 plasmids (data not shown). In addition, β-gal/706–856 neither altered cell viability, morphology, or integrity upon expression in 293T cells (data not shown) nor inhibited expression of the transfected human CD4 gene (Fig. 3B). These results collectively indicate that this mediator does not markedly alter global cellular functions or gene expression.

Effects of a cytoplasmic tail fragment on Gag expression

To understand whether the effect of β-gal/706–856 on depletion of Gag expression observed truly represent the effect of the cytoplasmic tail itself, a cytoplasmic tail fragment encoded by pRK5/706–856 as a 706–856/Flag fusion fragment (Lee et al., 2000) was assessed. As with β-gal/706–856, this cytoplasmic tail fragment reduced steady-state levels of Gag expressed (Fig. 4).

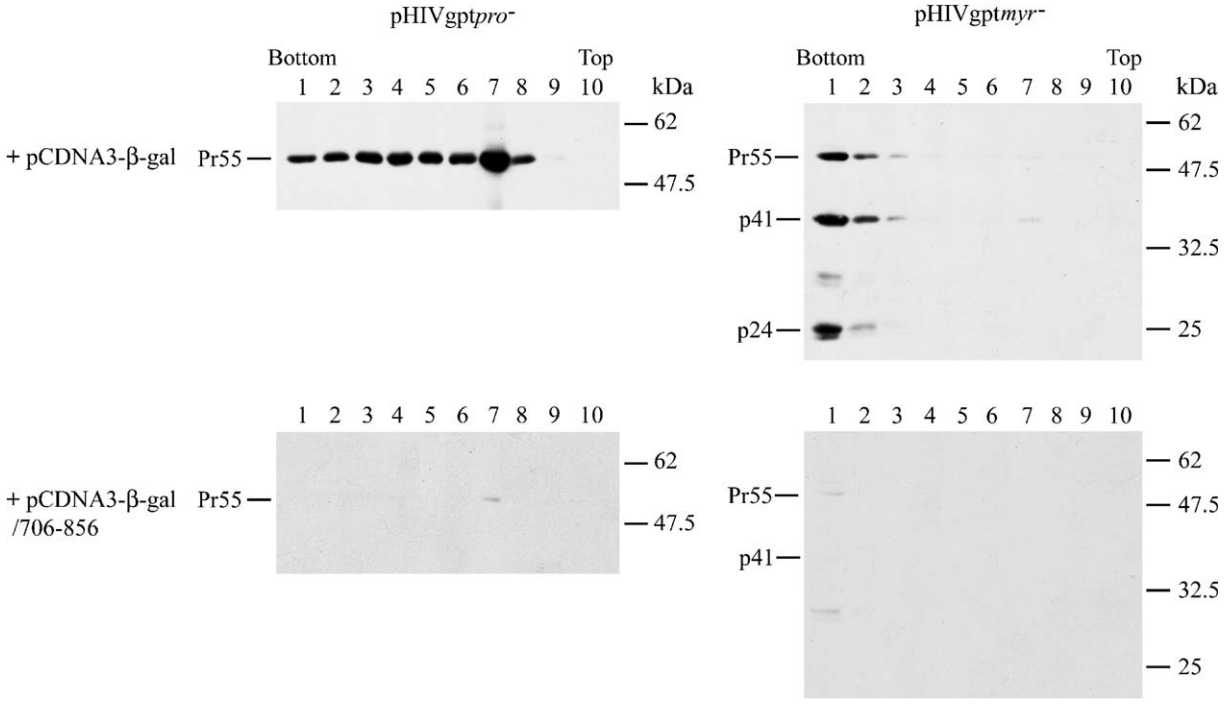

Fig. 2. Depletion of intracellular cytosolic and membrane-associated Gag complexes by β-gal/706–856. Cells cotransfected with pHIVgpt*pro*$^-$ or pHIVgpt*myr*$^-$ in the presence of β-gal plasmids as indicated were subjected to a membrane flotation assay. After fractionation, proteins in each fraction were precipitated by cold trichloroacetic acid, and then analyzed by Western blotting using Mab 183.

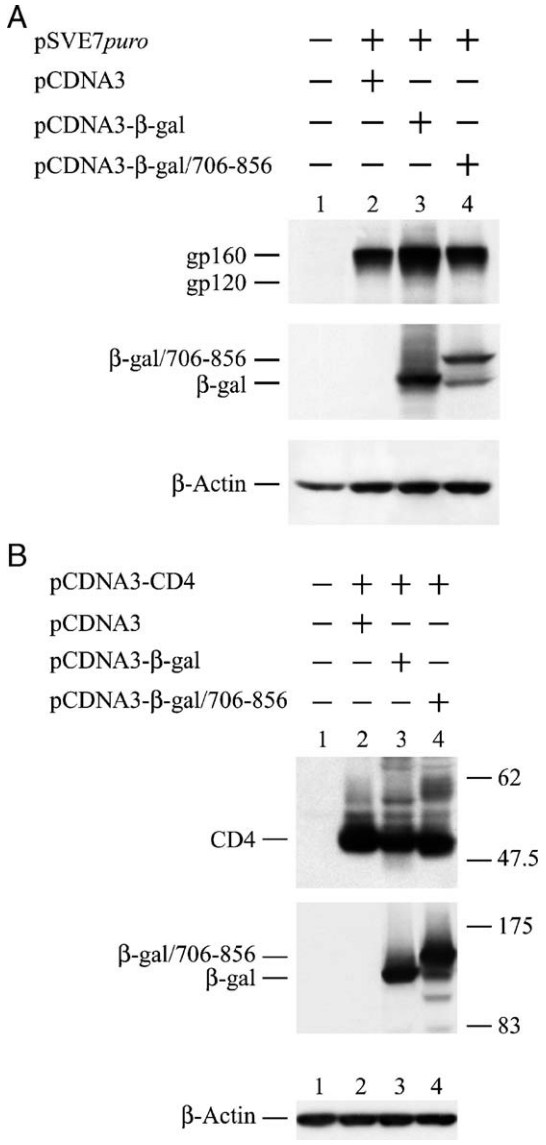

Fig. 3. Assessment of HIV-1 *env* and human CD4 gene expressions when coexpressed with β-gal/706–856. (A) 293T cells were cotransfected with pSVE7*puro* and pIIIex*tat* in the presence of each of the pCDNA3 plasmids as indicated. Cell lysates were assessed by Western blotting using Mabs 902, β-gal, or β-actin, respectively. (B) 293T cells were cotransfected with 5 μg of pCDNA3-CD4 and 5 μg of each of the pCDNA3 plasmids. Cell lysates were analyzed by Western blotting using SIM2, a Mab specific for CD4, and anti-β-gal, or anti-β-actin Mab, respectively.

Molecular interactions between Gag, and β-gal/706–856

We previously demonstrated that assessment of interactions between Gag and a cytoplasmic tail fusion protein by the detergent-containing, sucrose gradient ultracentrifugation method as previously described by Wyma et al. (2000) can detect authentic Env–Gag interactions (Chan et al., 2004). To further prove the fidelity of this method in detecting stable interaction between Gag and the cytoplasmic tail fusion protein, we determined if stable interactions exist between the native Env and Gag. Cell-free, immature viral particles obtained from Pr55 Gag and Env coexpression were layered onto a linear 30 to 70% (wt/vol) sucrose gradient with or without a layer of 1% Triton X-100 placed at the top of the gradient. Upon centrifugation, the immature virions pass through the layer of detergent and sediment to their equilibrium density in the sucrose gradient. gp160 and gp41 remained associated with Gag to a peak in fractions 8–10 in a gradient lacking detergent (Fig. 5A, top panel), representing isolation of intact viral particles. In a gradient containing detergent, the peak of Pr55 for the immature cores was detected in fractions 2 to 4 of the gradient (Fig. 5A, middle panel). The majority of Env and gp41 still remained associated with the Gag core in fractions 2–4 although some forms of gp160 and gp41 were also detected in top fractions of the gradient (Fig. 5A, middle panel). These top fractions of Env might have lost their ability to interact with Gag during treatment of the virus with Triton X-100 or ultracentrifugation. When cell lysates containing Env alone were analyzed, gp160 and gp41 were separately detected with peaks in fraction 8 and fractions 10 and 11, respectively (Fig. 5A, bottom panel). This approach thus provides a readily available assay to address detergent-resistant, molecular interactions between Gag and β-gal/706–856.

When lysates containing β-gal and β-gal/706–856 were analyzed, both β-gal and β-gal/706–856 were detected with a peak at fraction 9 (Fig. 5B). When virions obtained from cells cotransfected with pHIVgpt*pro*$^-$ and either β-gal or β-gal/706–856 were analyzed, a fraction of β-gal/706–856, but not β-gal, was associated with the Gag core in bottom fractions of the gradient (Fig. 5C). Similarly, the 706–856/Flag fragment was

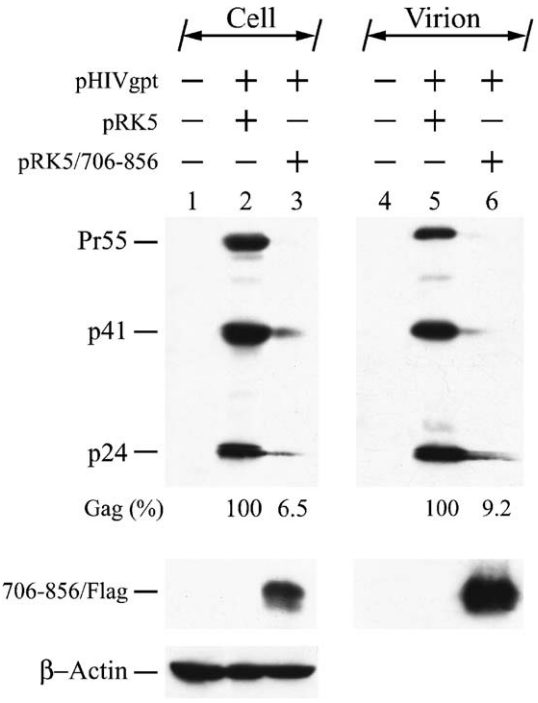

Fig. 4. Effect of a cytoplasmic tail fragment on Gag expression. 293T cells were cotransfected with 10 μg of pHIVgpt together with 10 μg of pRK5 or pRK5/706–856 as indicated. Cell and virion lysates were analyzed by Western blotting using Mabs 183, Chessie 8, and β-actin, respectively. The relative expression levels of Gag in cells and virions are also indicated.

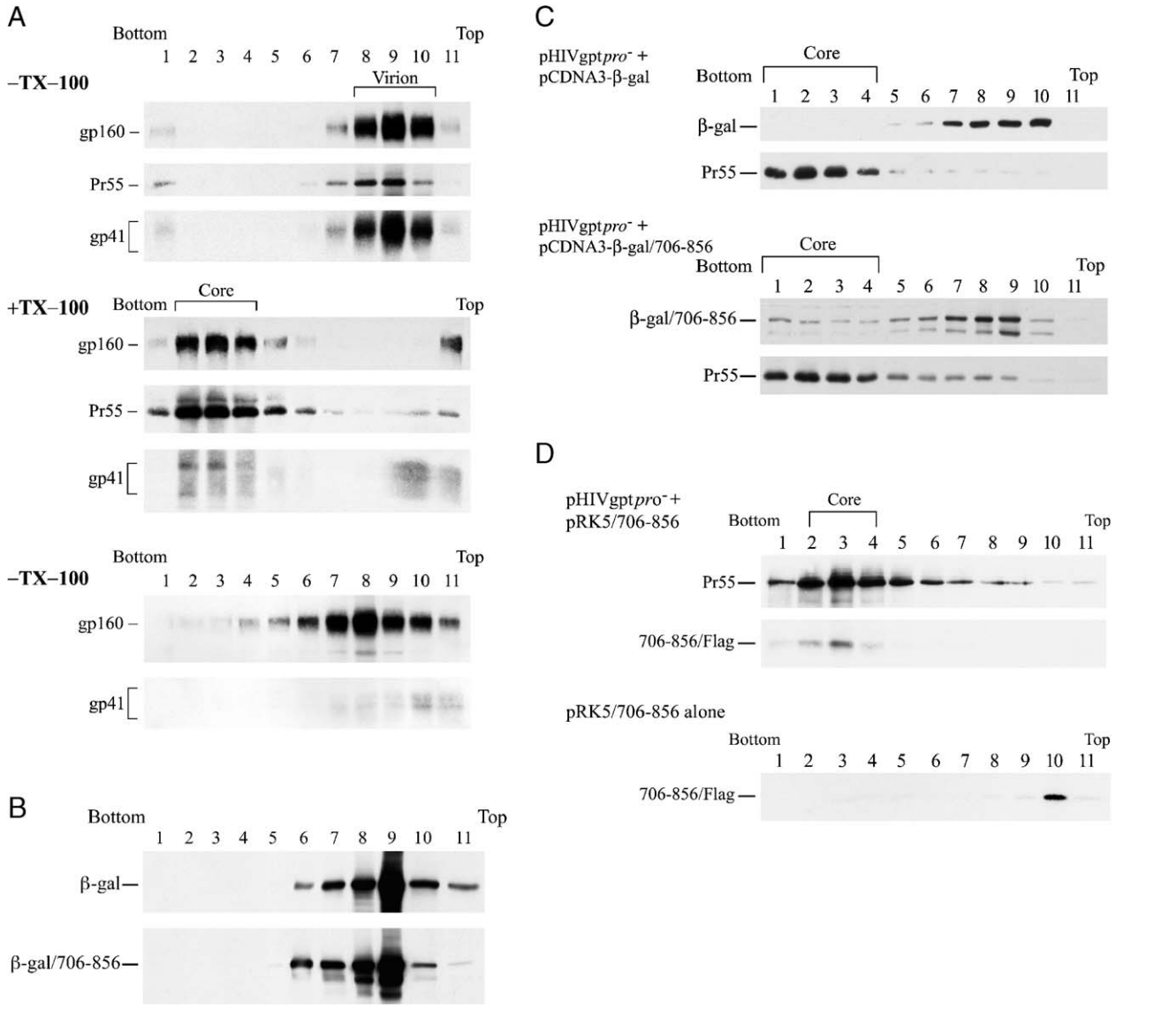

Fig. 5. Analyses of viral protein–protein interactions by sucrose gradient equilibrium ultracentrifugation. (A) Examination of Gag–Env interactions. Concentrated virions obtained from 293T cells cotransfected with pCMV*gag*, pSVE7*puro*, and pIIIex*tat* were analyzed by sucrose gradient ultracentrifugation which did (middle panel) or did not contain (top panel) a layer of 1% Triton X-100. Lysates containing Env were also analyzed by a sucrose gradient without detergent (bottom panel). (B) Sucrose gradient analysis of β-gal and β-gal/706–856. Cell lysates containing β-gal or β-gal/706–856 were analyzed by sucrose gradient containing detergent. (C) Characterization of Gag-β-gal/706–856 interactions. Virions obtained from cells cotransfected with 15 μg of pHIVgpt*pro*⁻ and 3.75 μg each of the β-gal or β-gal/706–856 plasmids were analyzed by sucrose gradients containing detergent. (D) Interaction between Gag and the 706–856/Flag fragment. Virions obtained from cells coexpressing Gag and 706–856/Flag or cell lysates containing 706–856/Flag were analyzed by sucrose gradients containing detergent. In the top and middle panels of (A), after fractionation, viral particles in each fraction were ultracentrifuged and analyzed by Western blotting. In the bottom panels of A–D, samples in each fraction were precipitated with trichloroacetic acid and then analyzed by Western blotting.

also specifically associated with the immature Gag core in bottom fractions of the gradient (Fig. 5D). These results together indicate that the cytoplasmic tail, per se, forms a detergent-resistant, complex with the Gag core.

Confocal microscopy of coexpressed viral proteins

Confocal immunofluorescence analyze were then performed to assess the intracellular localization of Gag and the fusion protein. As we previously reported (Chen et al., 2001), overexpression of cytosolic β-gal exhibited cytoplasmic staining (Fig. 6A, first panel) while β-gal/706–856 was predominantly located in the perinuclear region (Fig. 6A, second panel). Gag was localized in the entire cytoplasm (Fig. 6A, third panel). Gag and β-gal were both distributed in the cytoplasm when coexpressed, but they were not completely stained in the same regions (Fig. 6B, top panel). Gag and β-gal/706–856 were colocalized as aggregated structures in the perinuclear and cytoplasmic regions when coexpressed (Fig. 6B, bottom panel).

To determine whether Gag and β-gal/706–856 are colocalized in the ER, co-staining with an antibody directed against

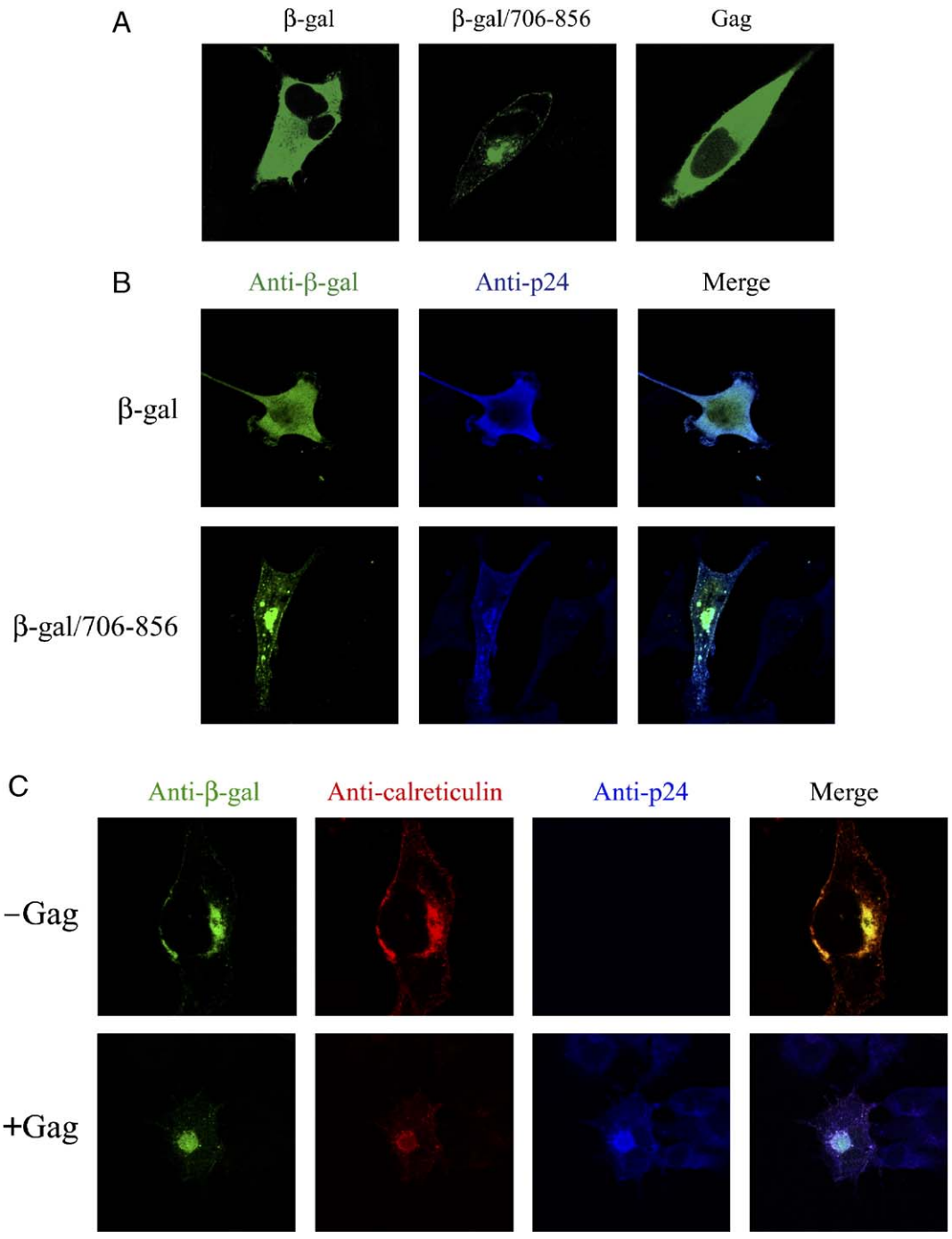

Fig. 6. Confocal immunofluorescence microscopy of coexpressed viral proteins. (A) HeLa cells grown on coverslips in 24-well plates were transfected with 3 μg each of pCDNA3-β-gal, pCDNA3-β-gal/706–856, or pHIVgpt*pro*$^{-}$ as indicated. Transfected cells were incubated with Mab anti-β-gal (first and second panels) and rabbit anti-p25/p24 (third panel), respectively. After incubation with appropriate FITC-labeled secondary antibodies, cells were examined by confocal microscopy. (B) HeLa cells were cotransfected with 1 μg each of the β-gal or β-gal/706–856 plasmid along with 1 μg of pHIVgpt*myr*$^{-}$. Transfected cells were incubated with Mab anti-β-gal and rabbit anti-p25/p24. After successive incubations with fluorescence-labeled secondary antibodies, cells were examined by confocal microscopy. (C) Cells were cotransfected with 1 μg of pCDNA3-β-gal/706–856 in the presence or absence of 1 μg of pHIVgpt*myr*$^{-}$. Transfected cells were successively incubated with anti-β-gal Mab, rabbit anti-p25/p24, goat anti-calreticulin, and appropriate fluorescence-labeled secondary antibodies; then cells were processed for confocal microscopy.

calreticulin, an ER marker, was performed. In the absence of Gag expression, β-gal/706–856 was colocalized with calreticulin (Fig. 6C, top panel), indicating its localization in the ER. When coexpressed with Gag, β-gal/706–856 was colocalized with Gag and calreticulin as large aggregates or punctate structures in the perinuclear or cytoplasmic regions (Fig. 6C, bottom panel), indicating that β-gal/706–856 specifically interacts with and directs Gag to perinuclear cytoplasmic regions. However, the ER staining pattern differed from that when β-gal/706–856 was expressed alone (Fig. 6C), suggesting that the coexpression of Gag and β-gal/706–856 may affect the structures or integrity of the ER.

Degradation of Gag mediated by β-gal/706–856

We then determined the mechanism underling downregulation of Gag expression by the cytoplasmic tail fusion protein. When 293T cells cotransfected with a fixed amount of pHIVgpt*myr*$^-$ in the presence of increasing amounts of β-gal or β-gal/706–856 plasmids were metabolically labeled with [^{35}S]methionine for 15 min or overnight, β-gal/706–856 decreased Gag expression in a dose-dependent manner (Fig. 7A), suggesting that β-gal/706–856 inhibits Gag translation and/or promotes Gag degradation. In vitro coupled transcription/translation reactions using a 1:1 molar ratio of T7 promoter-driven Gag and β-gal/705–856 plasmids showed that β-gal/705–856 did not affect Gag translation in the presence or absence of microsomal membranes (data not shown).

Next, a pulse-chase analysis, which assesses the turnover rate of newly synthesized molecules, was performed. Gag was turned over with faster kinetics when coexpressed with β-gal/705–856 than with β-gal (Fig. 7B). In addition, chasing with a translational inhibitor, cycloheximide (Mulder and Muesing, 2000), which monitors the turnover of preexisting proteins, showed that the turnover rate of Gag was faster with β-gal/706–856 coexpression than with β-gal coexpression, and that the degree in Gag degradation was dependent on the amount of the β-gal/706–856 plasmid used in cotransfection (Fig. 7C). Similarly, 706–856/Flag also enhanced Gag degradation in a time-dependent manner (Fig. 7D).

Discussion

We demonstrate herein that an HXB2 strain-derived Env cytoplasmic tail fusion protein, β-gal/706–856, depletes intracellular Gag molecules (Fig. 1) in a mediator dose-dependent manner (Figs. 1D and 7A). The depletion effect of this modulator on Gag expression was specific since this modulator did not affect steady-state expression of Env or CD4 (Fig. 3). A cytoplasmic tail fragment, 706–856/Flag, also reduced steady-state Gag expressions (Fig. 4). The action of the cytoplasmic tail-mediated reduction in steady-state Gag expression proceeded via time-dependent and mediator dose-dependent degradation when unmyristylated Gag was analyzed (Fig. 7). Although there is no direct evidence for the instability of myristylated Gag, myristylated Gag was still depleted when coexpressed with cytoplasmic tail fragments (Figs. 1A, B, and 4), it is likely that depletion of myristylated Gag by cytoplasmic tail fragments may still occur via a degradation pathway.

The results of confocal microscopy showed that β-gal/706–856, but not β-gal, specifically interacted with and directed Gag to perinuclear cytoplasmic regions, where an ER marker calreticulin also resided, to form aggregated complexes (Fig. 6). Sucrose gradient ultracentrifugation analyses also demonstrated detergent-resistant, stable interactions between Gag and the cytoplasmic tail fragments (Fig. 5). These results suggest that interactions of Gag with the cytoplasmic tail fusion protein and the targeting of Gag to an intracellular site are required for β-gal/706–856-mediated Gag depletion.

Different regions or sequences located in the C-terminal two-thirds segment of the Env cytoplasmic domain of primate immunodeficiency viruses have been implicated in interactions with Gag (Celma et al., 2001; Freed and Martin, 1995, 1996; Hourioux et al., 2000; Murakami and Freed, 2000). We previously showed that fusion proteins containing the cytoplasmic domain or each of the LLP motifs is colocalized with the ER markers (Chen et al., 2001). The present studies showed that β-gal/706–856 redirects Gag to an intracellular compartment, where calreticulin is also located, to form aggregated structures (Fig. 6). A structure called an "aggresome" has been defined as a pericentriolar, membrane-free, cytoplasmic inclusion composed of aggregated, misfolded proteins surrounded by disorganized filaments (Johnston et al., 1998). Formation of aggresomes is a general cellular response when the capacity of cells to degrade misfolded proteins is exceeded. It is likely that the vesicles or bodies containing the cytoplasmic tail fragment and Gag may represent aggresomes where altered Gag structures have accumulated.

We previously showed that β-gal/706–856 is rapidly associated with the membrane fraction after synthesis in a pulse-chase study (data not shown). Other studies also showed that interactions of LLP sequences with membranes proceed in a rapid mode (Miller et al., 1993; Srinivas et al., 1992). This may explain why Gag rapidly degrades when coexpressed with β-gal/706–856 even during the 10-min or 15-min labeling time (Fig. 7A) since Gag may rapidly interact with β-gal/706–856 after biosynthesis. Nevertheless, metabolically labeled and preexisting, unlabeled Gag molecules undergo time-dependent degradation (Figs. 7B, C, and D).

We show here that the interplay between Gag and β-gal/706–856 can modulate Gag expression. In the context of Env and β-gal/706–856 coexpression, β-gal/706–856 does not affect Env synthesis (Fig. 3A), indicating that the interaction of β-gal/706–856 with Env, presumably via cytoplasmic tail intersubunit interactions, does not destabilize the Env-β-gal/706–856 complex. However, in the context of Gag and β-gal/706–856 coexpression, the structurally altered Gag-β-gal/706–856 complexes formed after biosynthesis are unstable and subsequently degrade intracellularly by an as yet uncharacterized intracellular degradation pathway. Alternatively, β-gal/706–856 may somehow interfere with the multimerization, assembly, or intracellular trafficking processes of Gag, rendering Gag assembly intermediate complexes susceptible to degradation.

In the present study, we demonstrate a novel mode of downregulation of HIV-1 Gag expression by a cytoplasmic domain fusion protein, which can serve as a module to control the expressions of Gag, thus regulating HIV-1 Gag assembly/budding. Since Gag expression is crucial for morphogenesis and the formation of an infectious virus, our study also has implications for diverting Gag from its normal maturation and assembly/budding pathway to an intracellular degradation route. The results may help design a genetic antiviral strategy to control the maturation process of HIV-1 Gag protein.

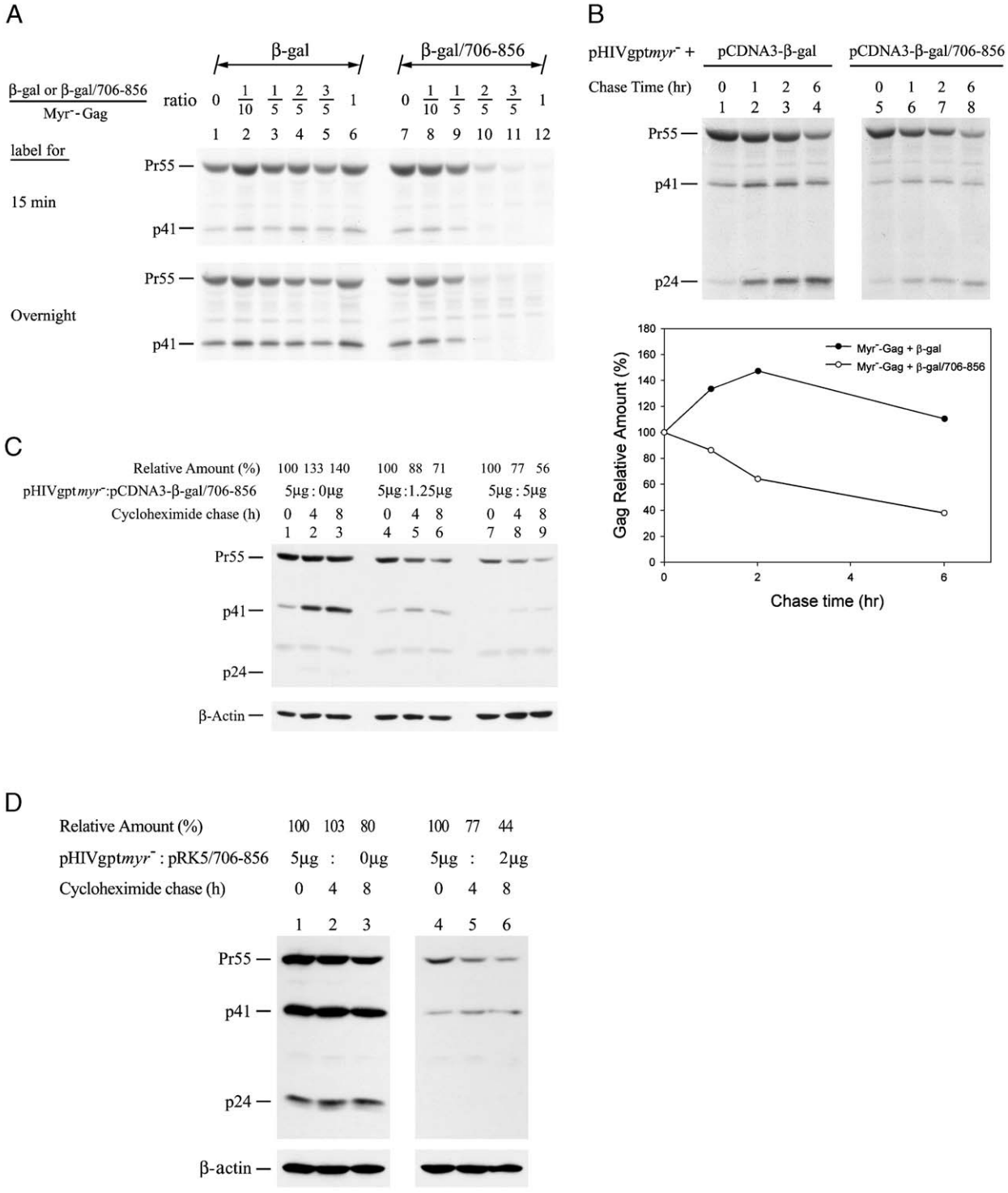

Fig. 7. Promotion of Gag degradation by cytoplasmic tail fusion proteins. (A) 293T cells were cotransfected with 5 μg of pHIVgpt*myr*⁻ together with the β-gal or β-gal/706–856 plasmid at different molar ratios of Gag to β-gal or β-gal/706–856 plasmids as indicated. pCDNA3 was added to adjust the total amounts of DNA in all transfections to be the same. Transfected cells were metabolically labeled with [^{35}S]methionine for 15 min (top panel) or overnight (bottom panel). Cell lysates were immunoprecipitated with AIDS patients' antisera preadsorbed onto protein A-Sepharose 4B beads, followed by SDS-PAGE. (B) 293T cells cotransfected with 5 μg of pHIVgpt*myr*⁻ along with 2 μg each of the β-gal and β-gal/706–856 plasmids were metabolically labeled for 10 min and then chased with excess cold methionine for different time points. Cell lysates were immunoprecipitated, and the immune complexes were resolved by SDS-PAGE (top panel). The dried gels were scanned and quantitated as described under Materials and methods. The relative percentages of the total radioactivity of Gag proteins at each chase time to that of the Gag proteins at chase time zero were plotted (bottom panel). (C) Cells were cotransfected with 5 μg of pHIVgpt*myr*⁻ and the indicated amounts of pCDNA3-β-gal/706–856. pCDNA3-β-gal was added to the transfection mixtures to maintain the same amount of total plasmids in each transfection. A cycloheximide chase was performed, and cell lysates obtained at different time points after the chase were analyzed by Western blotting. Photos of ECL blots were scanned and quantitated, and the total intensities of Gag for different chase periods are expressed as percentages of those of Gag at a chase time of zero. (D) Cells were cotransfected with 5 μg of pHIVgpt*myr*⁻ and 2 μg of pRK5 (lanes 1 to 3) or pRK5/706–856 (lanes 4 to 6), and the cycloheximide chase was performed as described in panel C.

Materials and methods

Cells, hybridomas, and antibodies

HEK293T and HeLa cells were cultured in Dulbecco's modified Eagle's medium supplemented with 10% heat-inactivated fetal bovine serum (FBS). Hybridoma 902, Chessie 8, and 183 (clone H12-5C) were described previously (Lee et al., 2002). SIM2 is a hybridoma producing a Mab that recognizes human CD4. All of these hybridomas were maintained in RPMI-1640 containing 10% FBS. Rabbit antiserum to HIV-1 p25/p24 was previously described (Chen et al., 1998). Mabs directed against β-gal and β-actin were purchased from Promega and Sigma, respectively. Affinity-purified goat antibody directed against the C-termini of human calreticulin was obtained from Santa Cruz Biotechnology, Inc. (Santa Cruz, CA).

Construction of plasmids

pCDNA3-CD4 was constructed by cloning the *Eco*RI–*Xba*I fragment isolated from a human CD4 plasmid, pBS-CD4 (Shaw et al., 1989), into the corresponding sites in pCDNA3 (Invitrogen, Carlsbad, CA).

Plasmid DNA transfection

293T cells were transfected with plasmids using a standard calcium phosphate coprecipitation method as previously described (Chen et al., 1998, 1999). For Env expression, 293T cells were cotransfected with 5 μg of pSVE7*puro* and 3 μg of an HIV-1 LTR-directed Tat expression plasmid pIIIex*tat* in the presence of 5 μg of pCDNA3-β-gal/706–856. When the effect of β-gal/706–856 on Gag expression from pHIVgpt clones was examined, 10 μg each of the pCDNA3-β-gal/706–856 and pHIVgpt clones was used for cotransfection unless otherwise indicated. For sucrose gradient ultracentrifugation, 293T cells were transfected with 10 μg of pCMV*gag* in the presence of 10 μg of pSVE7*puro* and 3 μg of pIIIex*tat*. Alternatively, cells were cotransfected with pHIVgpt*pro*$^{-}$ in the presence of pCDNA3-β-gal or pCDNA3-β-gal/706–856 at the plasmid ratios indicated in each experiment. HeLa cells were transfected with plasmid DNAs by the lipofectamine transfection method (Life Technologies, Rockville, MD).

Virus preparation and Western blot analysis

Two days after transfection, cell-free virions were isolated through a 20% (wt/wt) sucrose cushion, and equal volumes of cell and viral lysates were analyzed by SDS-PAGE and Western blotting. The membrane blots were incubated with appropriate primary and secondary antibodies followed by enhanced chemiluminescent (ECL) detection. For quantitation, ECL photos of the blots within the linear range of the film were scanned using a Microtek ScanMarker 8700 (Carson, CA) and quantitated using MetaMorph software (Universal Imaging, Downing Town, PA). The relative percentages of Gag levels in cells and virions are shown below each lane of the Western blots.

Membrane flotation assay and isolation of HIV-1 core structures

For membrane flotation, washed transfected cells were sonicated twice in 0.5 ml of hypotonic TE buffer (10 mM Tris–HCl, pH 7.5, containing 1 mM EDTA) supplemented with a complete protease inhibitor cocktail (Roche Molecular Biochemicals; Mannheim, Germany) and 10% (wt/vol) sucrose on ice using an Ultrasonic Processor Model W-375 (Ultrasonics; Farmingdale, NY) with output power of 20%–30%, each time for 15 s. After centrifugation at 1000 × *g* and 4 °C for 10 min, the postnuclear fractions were subjected to the membrane flotation assay as previously described (Chen et al., 2001). Briefly, 0.25 ml of postnuclear supernatants were mixed with 1.25 ml of 85.5% (wt/vol) sucrose, and placed at the bottom of a Beckman SW41 ultracentrifuge tube, and then 7 ml of 65% (wt/vol) sucrose and 3.25 ml of 6% (wt/vol) sucrose (all prepared in TE buffer) were successively loaded into the tube. The gradients were centrifuged at 100,000 × *g* for 18 h at 4 °C. After ultracentrifugation, samples were fractionated from the bottom of the gradients, and 1.2 ml per fraction was collected. Immature cores were isolated from cell-free, concentrated viruses according to a previously described procedure (Wyma et al., 2000) except that 0.45 ml of 15% sucrose (wt/vol) containing 1% Triton X-100 was overlaid on the top of the 30% to 70% (wt/vol) linear density sucrose gradients (Chan et al., 2004). The gradients were centrifuged at 100,000 × *g* for 16 h at 4 °C. After fractionation, the samples in each fraction were diluted to a total volume of 4 ml with STE buffer (10 mM Tris–HCl, pH 7.4, containing 100 mM NaCl and 1 mM EDTA) and then centrifuged at 50,000 rpm and 4 °C for 30 min in an SW60 rotor to pellet the viruses. Alternatively, samples were precipitated with 10% cold trichloroacetic acid. The viral proteins were then analyzed by Western blotting.

Confocal immunofluorescence microscopic studies

Transfected HeLa cells were fixed by 4% paraformaldehyde, permeabilized by 0.25% Triton X-100, and then separately incubated with the appropriate primary antibodies. After successive incubation with 1:100 dilutions of fluorescein isothiocyanate (FITC)-, tetramethylrhodamine isothiocyanate-, and Cy5-conjugated secondary antibodies directed against each species from which the primary antibodies were generated, the immunostained cells were analyzed by confocal microscopy as previously described (Chen et al., 2001).

Metabolic labeling, pulse-chase, and immunoprecipitation

One day after transfection, 293T cells were metabolically labeled with [^{35}S]methionine for the time as indicated or labeled for 30 min and chased with excess cold methionine as previously described (Lee et al., 2002). Cell lysates were immunoprecipitated with pooled AIDS patients' antisera

preadsorbed onto protein A-Sepharose 4B beads, extensively washed, and separated by SDS-PAGE followed by fluorography as previously described (Chan et al., 2004). The dried gels in Fig. 7B were scanned and quantitated using a Packard Instant Imager, model A202401 (Packard Instrument; Meriden, CT) for the radioactivity of the Pr55, p41, and p24 species. Pr55, MA, and CA of the HXB2 virus contain 16, 1, and 11 Met residues, respectively. The radioactivities of the Pr55, p41, and p24 species were calibrated by multiplying the radioactivity of each species by factors of 16/16, 16/12, and 16/11, respectively.

Cycloheximide chase

Sixteen hours after transfection, 293T cells were treated with cycloheximide (Sigma) at a final concentration of 100 μg/ml. Cells lysates were harvested at sequential time points after treatment, and analyzed by Western blotting.

Acknowledgments

The following reagents were obtained through the AIDS Research and Reference Reagent Program, Division of AIDS, NIAID, NIH, USA: SIM2 hybridoma from J. Hildreth, pHIVgpt from K. Page and D. Littman, and rabbit anti-p25/p24 from K. Steimer. We are grateful to J. K. Rose for providing pBS-CD4 and C.-T. Wang for helpful discussions and providing the pCMV*gag* and pHIVgpt-derived *myr*$^-$ and *pro*$^-$ constructs.

This work was supported by grants from the National Health Research Institute (NHRI-EX92-9136SN, NHRI-EX93-9136SN, and NHRI-EX94-9431SI) and Academia Sinica (AS91IBMS3PP), Taipei, Taiwan, Republic of China.

References

Berlioz-Torrent, C., Shacklett, B.L., Erdtmann, L., Delamarre, L., Bouchaert, I., Sonigo, P., Dokhelar, M.C., Benarous, R., 1999. Interactions of the cytoplasmic domains of human and simian retroviral transmembrane proteins with components of the clathrin adaptor complexes modulate intracellular and cell surface expression of envelope glycoproteins. J. Virol. 73, 1350–1361.

Blot, G., Janvier, K., Le Panse, S., Benarous, R., Berlioz-Torrent, C., 2003. Targeting of the human immunodeficiency virus type 1 envelope to the *trans*-Golgi network through binding to TIP47 is required for env incorporation into virions and infectivity. J. Virol. 77, 6931–6945.

Boge, M., Wyss, S., Bonifacino, J.S., Thali, M., 1998. A membrane-proximal tyrosine-based signal mediates internalization of the HIV-1 envelope glycoprotein via interaction with the AP-2 clathrin adaptor. J. Biol. Chem. 273, 15773–15778.

Bryant, M., Ratner, L., 1990. Myristylation-dependent replication and assembly of human immunodeficiency virus 1. Proc. Natl. Acad. Sci. U.S.A. 87, 523–527.

Celma, C.C., Manrique, J.M., Affranchino, J.L., Hunter, E., Gonzalez, S.A., 2001. Domains in the simian immunodeficiency virus gp41 cytoplasmic tail required for envelope incorporation into particles. Virology 283, 253–261.

Chan, W.-E., Wang, Y.-L., Lin, H.-H., Chen, S.S.-L., 2004. Effect of extension of the cytoplasmic domain of human immunodeficiency type 1 virus transmembrane protein gp41 on virus replication. J. Virol. 78, 5157–5169.

Chen, S.S.-L., Ferrante, A.A., Terwilliger, E.F., 1996. Characterization of an envelope mutant of HIV-1 that interferes with viral infectivity. Virology 226, 260–268.

Chen, S.S.-L., Lee, S.-F., Hao, H.-J., Chuang, C.-K., 1998. Mutations in the leucine zipper-like heptad repeat sequence of human immunodeficiency virus type 1 gp41 dominantly interfere with wild-type virus infectivity. J. Virol. 72, 4765–4774.

Chen, S.S.-L., Lee, S.-F., Chuang, C.-K., Raj, V.S., 1999. *trans*-Dominant interference with human immunodeficiency virus type 1 replication and transmission in $CD4^+$ cells by an envelope double mutant. J. Virol. 73, 8290–8302.

Chen, S.S.-L., Lee, S.-F., Wang, C.-T., 2001. Cellular membrane-binding ability of the C-terminal cytoplasmic domain of human immunodeficiency virus type 1 envelope transmembrane protein gp41. J. Virol. 75, 9925–9938.

Cosson, P., 1996. Direct interaction between the envelope and matrix proteins of HIV-1. EMBO J. 15, 5783–5788.

Freed, E.O., 1998. HIV-1 gag proteins: diverse functions in the virus life cycle. Virology 251, 1–15.

Freed, E.O., Martin, M.A., 1995. Virion incorporation of envelope glycoproteins with long but not short cytoplasmic tails is blocked by specific, single amino acid substitutions in the human immunodeficiency virus type 1 matrix. J. Virol. 69, 1984–1989.

Freed, E.O., Martin, M.A., 1996. Domains of the human immunodeficiency virus type 1 matrix and gp41 cytoplasmic tail required for envelope incorporation into virions. J. Virol. 70, 341–351.

Garnier, L., Bowzard, J.B., Wills, J.W., 1998. Recent advances and remaining problems in HIV assembly. AIDS 12 (Suppl. A), S5–S16.

Garoff, H., Hewson, R., Opstelten, D.J., 1998. Virus maturation by budding. Microbiol. Mol. Biol. Rev. 62, 1171–1190.

Gelderblom, H.R., Hausmann, E.H., Ozel, M., Pauli, G., Koch, M.A., 1987. Fine structure of human immunodeficiency virus (HIV) and immunolocalization of structural proteins. Virology 156, 171–176.

Gottlinger, H.G., Sodroski, J.G., Haseltine, W.A., 1989. Role of capsid precursor processing and myristoylation in morphogenesis and infectivity of human immunodeficiency virus type 1. Proc. Natl. Acad. Sci. U.S.A. 86, 5781–5785.

Hermida-Matsumoto, L., Resh, M.D., 2000. Localization of human immunodeficiency virus type 1 Gag and Env at the plasma membrane by confocal imaging. J. Virol. 74, 8670–8679.

Hill, C.P., Bancroft, D.W.P., Christensen, A.M., Sundquist, W.I., 1996. Crystal structures of the trimeric human immunodeficiency virus type 1 matrix protein: implications for membrane association and assembly. Proc. Natl. Acad. Sci. U.S.A. 93, 3099–3104.

Hourioux, C., Brand, D., Sizaret, P.Y., Lemiale, F., Lebigot, S., Barin, F., Roingeard, P., 2000. Identification of the glycoprotein 41(TM) cytoplasmic tail domains of human immunodeficiency virus type 1 that interact with Pr55 (Gag) particles. AIDS Res. Hum. Retroviruses 16, 1141–1147.

Johnston, J.A., Ward, C.L., Kopito, R.R., 1998. Aggresomes: a cellular response to misfolded proteins. J. Cell Biol. 143, 1883–1898.

Lee, S.-F., Wang, C.-T., Liang, J.Y.-P., Hong, S.-L., Huang, C.-C., Chen, S.S.-L., 2000. Multimerization potential of the cytoplasmic domain of the human immunodeficiency virus type 1 transmembrane glycoprotein gp41. J. Biol. Chem. 275, 15809–15819.

Lee, S.-F., Ko, C.-Y., Wang, C.-T., Chen, S.S.-L., 2002. Effect of point mutations in the N terminus of the lentivirus lytic peptide-1 sequence of human immunodeficiency virus type 1 transmembrane glycoprotein gp41 on Env stability. J. Biol. Chem. 277, 15363–15375.

Massiah, M.A., Starich, M.R., Paschall, C., Summer, M.F., Christensen, A.M., Sundquist, W.I., 1994. Three-dimensional structure of the human immunodeficiency virus type 1 matrix protein. J. Mol. Biol. 244, 198–223.

Matthews, S., Barlow, P., Boyd, J., Barton, G., Russell, R., Mills, H., Cunningham, M., Meyers, N., Burns, N., Clark, N., Kingsman, S., Kingsman, A., Campbell, I., 1994. Structural similarity between the p17 matrix protein of HIV-1 and interferon-γ. Nature (London) 370, 666–668.

Micoli, K.J., Pan, G., Wu, Y., Williams, J.P., Cook, W.J., McDonald, J.M., 2000. Requirement of calmodulin binding by HIV-1 gp160 for enhanced FAS-mediated apoptosis. J. Biol. Chem. 275, 1233–1240.

Miller, M.A., Cloyd, M.W., Liebmann, J., Rinaldo Jr., C.R., Islam, K.R., Wang, S.Z.S., Mietzner, T.A., Montelaro, R.C., 1993. Alterations in cell membrane permeability by the lentivirus lytic peptide (LLP-1) of HIV-1 transmembrane protein. Virology 196, 89–100.

Mulder, L.C., Muesing, M.A., 2000. Degradation of HIV-1 integrase by the N-end rule pathway. J. Biol. Chem. 275, 29749–29753.

Murakami, T., Freed, E.O., 2000. Genetic evidence for an interaction between human immunodeficiency virus type 1 matrix and α-helix 2 of the gp41 cytoplasmic tail. J. Virol. 74, 3548–3554.

Nermut, M.V., Hockley, D.J., Jowett, J.B.M., Jones, I.M., Garrequ, M., Thomas, D., 1994. Fullerene-like organization of HIV gag-protein shell in virus-like particles produced by recombinant baculovirus. Virology 198, 288–296.

Ohno, H., Aguilar, R.C., Fournier, M.C., Hennecke, S., Cosson, P., Bonifacino, J.S., 1997. Interaction of endocytic signals from the HIV-1 envelope glycoprotein complex with members of the adaptor medium chain family. Virology 238, 305–315.

Ono, A., Freed, E.O., 1999. Binding of human immunodeficiency virus type 1 Gag to membrane: role of the matrix amino terminus. J. Virol. 73, 4136–4144.

Page, K.A., Landau, N.R., Littman, D.R., 1990. Construction and use of a human immunodeficiency virus vector for analysis of virus infectivity. J. Virol. 64, 5270–5276.

Paillart, J.C., Gottlinger, H.G., 1999. Opposing effects of human immunodeficiency virus type 1 matrix mutations support a myristyl switch model of gag membrane targeting. J. Virol. 73, 2604–2612.

Pan, Z., Radding, W., Zhou, T., Hunter, E., Mountz, J., McDonald, J.M., 1996. Role of calmodulin in HIV-potentiated Fas-mediated apoptosis. Am. J. Pathol. 149, 903–910.

Rao, Z., Belyaev, A.S., Fry, E., Roy, P., Jones, I.M., Stuart, D.L., 1995. Crystal structure of SIV matrix antigen and implications for virus assembly. Nature (London) 378, 743–747.

Sakalian, M., Hunter, E., 1998. Molecular events in the assembly of retrovirus particles. Adv. Exp. Med. Biol. 440, 329–339.

Salzwedel, K., West Jr., J.T., Mulligan, M.J., Hunter, E., 1998. Retention of the human immunodeficiency virus type 1 envelope glycoprotein in the endoplasmic reticulum does not redirect virus assembly from the plasma membrane. J. Virol. 72, 7523–7531.

Schubert, U., Anton, L.C., Gibbs, J., Norbury, C.C., Yewdell, J.W., Bennink, J.R., 2000. Rapid degradation of a large fraction of newly synthesized proteins by proteasomes. Nature (London) 404, 770–774.

Shaw, A.S., Amrein, K.E., Hammond, C., Stern, D.F., Sefton, B.M., Rose, J.K., 1989. The lck tyrosine protein kinase interacts with the cytoplasmic tail of the CD4 glycoprotein through its unique amino-terminal domain. Cell 59, 627–636.

Spearman, P., Horton, R., Ratner, L., Kuli-Zade, I., 1997. Membrane binding of human immunodeficiency virus type 1 matrix protein in vivo supports a conformational myristyl switch mechanism. J. Virol. 71, 6582–6592.

Srinivas, S.K., Srinivas, R.V., Anantharamaiah, G.M., Segrest, J.P., Compans, R.W., 1992. Membrane interactions of synthetic peptides corresponding to amphipathic helical segments of the human immunodeficiency virus type-1 envelope glycoprotein. J. Biol. Chem. 267, 7121–7127.

Tritel, M., Resh, M.D., 2000. Kinetic analysis of human immunodeficiency virus type 1 assembly reveals the presence of sequential intermediates. J. Virol. 74, 5845–5855.

Vincent, M.J., Melsen, L.R., Martin, A.S., Compans, R.W., 1999. Intracellular interaction of simian immunodeficiency virus Gag and Env proteins. J. Virol. 73, 8138–8144.

Wang, C.T., Barklis, E., 1993. Assembly, processing, and infectivity of human immunodeficiency virus type 1 gag mutants. J. Virol. 67, 4264–4273.

Wang, C.T., Chou, Y.C., Chiang, C.C., 2000. Assembly and processing of human immunodeficiency virus Gag mutants containing a partial replacement of the matrix domain by the viral protease domain. J. Virol. 74, 3418–3422.

Wyma, D.J., Kotov, A., Aiken, C., 2000. Evidence for a stable interaction of gp41 with Pr55(Gag) in immature human immunodeficiency virus type 1 particles. J. Virol. 74, 9381–9387.

Wyss, S., Berlioz-Torrent, C., Boge, M., Blot, G., Honing, S., Benarous, R., Thali, M., 2001. The highly conserved C-terminal dileucine motif in the cytosolic domain of the human immunodeficiency virus type 1 envelope glycoprotein is critical for its association with the AP-1 clathrin adaptor. J. Virol. 75, 2982–2992.

Zhou, W., Resh, M.D., 1996. Differential membrane binding of the human immunodeficiency virus type 1 matrix protein. J. Virol. 70, 8540–8548.